

Structure and Energetics of the Water/NaCl(100) Interface

David P. Taylor, Wayne P. Hess, and Maureen I. McCarthy*

Environmental Molecular Sciences Laboratory, MS K1-96, Pacific Northwest National Laboratory, Richland, Washington 99352

Received: February 14, 1997[®]

A series of correlation-corrected periodic Hartree–Fock (PHF) calculations have been performed to evaluate the structure of a single layer of water adsorbed on NaCl(100). This work was motivated by differing experimental observations which assign the water/NaCl interface structure as either a monolayer, with a single adsorbate binding site, or a 4×2 bilayer model. Quantum mechanical binding energies were computed for several adsorbate/surface geometries corresponding to 1×1 and 2×1 monolayer structures and 4×2 bilayer structures. The calculations indicate that the binding energy per water molecule for the monolayer and bilayer models are very similar; the estimated PHF and correlation-corrected binding energies are 10 and 14 kcal/mol, respectively, for both models. When measured per unit surface area the 4×2 bilayer is energetically favored because it has a 50% greater packing density than the monolayer. The computed binding energies are consistent with experiment. These data show that the monolayer structure may be stable (or metastable) at low water coverages, but as the coverage is increased the bilayer structures become more favorable. The quantum mechanical data imply that the structure of the water/NaCl interface will be very sensitive to the sample preparation and experimental techniques used. The calculated binding energies for the 4×2 water bilayer geometries reveal the existence of many local minima on the potential energy surface which could result in the domaining of water on the NaCl(100) surface.

I. Introduction

The problem of how water interacts with sodium chloride and other salts is an active topic of research in surface physics and environmental chemistry.^{1–11} Sodium chloride surfaces have been shown to play a key role in heterogeneous chemical reactions that occur in the troposphere over the earth's oceans.¹² Most of the earth is covered with salt water, and ocean sprays carry sodium chloride, as well as water, into the atmosphere in large amounts. Airborne nitric oxide pollutants (NO₂, N₂O₅, ClONO₂) readily react with sodium chloride particles in the troposphere to form sodium nitrate and photochemically reactive chlorinated species.^{13–15} Understanding the structure, energetics, and reactivity of water on salt surfaces is key to modeling these environmental phenomena.

It is clear that the chemical reactivity of ionic crystal surfaces can be significantly altered by the presence of water.^{1,16} Determining the properties of specific salt/water interfaces is complicated because these materials tend to be “structure sensitive”; that is, the interface chemistry and physics are very dependent on the local geometry of individual surface sites. Different sample preparation techniques can produce variations in the atomic-scale surface topology, which can result in dramatic changes in the observed structure and reactivity of the interfaces. Several experimental^{1–5,7,8,10} and theoretical^{6,9–11} probes have been used to examine the water/NaCl(100) interface. These studies have reported two different types of structures (classified by the location of the water oxygens) for water adsorbed on NaCl(100). One proposed geometry is a (1×1) “monolayer” in which there is one water for each surface NaCl unit with the water oxygen atoms located in the vicinity of the surface sodium and all of the water dipoles oriented in the same direction.¹⁰ Another proposed geometry for water on NaCl(100) is a hexagonal (4×2) “bilayer” structure.^{5,6,11} Several (4×2) geometries are possible in which the water oxygens are

fixed and the hydrogen positions are varied corresponding to different water–water and water–surface orientations. These bilayer structures all contain 12 water molecules for every eight NaCl surface units (corresponding to 150% of the 1×1 coverage). A (2×1) monolayer structure containing two distinct water molecules for every two NaCl surface units has been proposed for the related system, water on MgO (001).¹¹

Reported experimental investigations on the water/NaCl interface have only been able to probe the positions of the oxygens, not the hydrogens. Different surface structures were reported depending on the experimental method and the sample preparation technique used. The (4×2) structures were observed using low-energy electron diffraction (LEED), X-ray photoemission spectroscopy (XPS), ultraviolet photoemission spectroscopy (UPS), and electron-energy loss spectroscopy (EELS) on thin NaCl films grown on Ge(100).^{4–7,11} The diffuseness in the reported LEED pattern may be indicative of multiple water–surface domains. A 4×2 water structure has also been detected with LEED on MgO(100).¹⁷ In contrast, the 1×1 monolayer structure was detected using He scattering on a NaCl crystal cleaved along ⟨100⟩ in vacuo.¹⁰ It is possible that infrared (IR) spectroscopy of water on the NaCl(100) surface may provide additional insight into the water–NaCl geometry as this method has been used to probe differences between monolayer and bilayer structures for ice interfaces.^{18–22} In addition to the differences in the reported structures, there is also a spread in the reported water–NaCl binding energies ranging from 10 to 15 kcal/mol.^{5,10}

Theoretical studies on the water/NaCl interface have also yielded different structures depending on the models and methods used to describe the system. Classical simulations using model potentials have predicted both the monolayer (1×1)¹⁰ and the bilayer (4×2)^{6,11} geometries. The results of calculations using a combined QM/MM method are consistent with the (1×1) monolayer structure.⁹ Ab initio periodic Hartree–Fock calculations have been used extensively to study

* Corresponding author. E-mail: mi_mccarthy@pnl.gov.

[®] Abstract published in *Advance ACS Abstracts*, September 1, 1997.

TABLE 1: Comparison of Adsorbate/Surface PHF Binding Energies and Distances for Water on Three-Layer and One-Layer Slabs of NaCl(100)^a

geometry	3-layer slab (oxygen–surface distance)	1-layer slab (oxygen–surface distance)
planar over sodium (see Table 2a)	−9.8 kcal/mol (2.5 Å)	−9.7 kcal/mol (2.5 Å)
over chlorine (see Table 2e)	−3.7 kcal/mol (3.5 Å)	−3.6 kcal/mol (3.5 Å)

^a Negative energies indicate bound geometries.

water on a related cubic material MgO(001).^{23–26} These studies probed the reactivity of flat terrace and defect sites in “(1×1)-like” structures but have not investigated (4×2) geometries.

The present work uses correlation-corrected periodic Hartree–Fock theory to investigate the energetics of (1×1) and (2×1) monolayer structures and several (4×2) bilayer geometries. Calculations on an extensive set of water–surface and water–water orientations yield insight into the relative stability of the different structures. These calculations directly probe the relative importance of water–water and water–surface interactions in determining the interface structure. This study was motivated by the fact that the empirical investigations on this system have only probed the water–oxygen overlayer positions (i.e. no direct empirical measurements have been made of the hydrogen positions, hence the water–water orientations are uncertain). Therefore, most of the calculations reported here fix the water oxygen positions in the empirically determined positions and vary water–water orientations in order to determine the overlayer structure.

II. Method

The ab initio electronic structure calculations were performed using periodic Hartree–Fock (PHF) theory²⁷ and correlation-corrected PHF theory^{28–30} as implemented in the program CRYSTAL.³¹ The NaCl(100) surface was modeled as a finite thickness slab (along the *z* direction), periodic along the in-plane coordinates (*x* and *y*) with an NaCl lattice constant of 5.78 Å.³² Earlier calculations on MgO(001) indicated that a three-layer slab was sufficient to describe the surface properties.^{23,24} Because of the increased size and complexity of the water/NaCl system the three-layer slab model was only used to compute the energetics of the (1×1) and (2×1) monolayer structures. Calculations on the monolayer structures indicated that the computed binding energies using a one-layer NaCl slab were within 0.2 kcal/mol of the values obtained using a three-layer slab (see Table 1). Reducing the slab thickness reduced the computational requirements, and hence, allowed us to probe the energetics of a systematic set of the more complex (4×2) structures. The (4×2) configurations contained 52 atoms (28 heavy atoms) with 456 basis functions and no symmetry. They were run on a Cray C90 and required 12 Gbytes of disk space, 20 MW of memory and 3 central processing unit hours, per point.

The plane group symmetry of NaCl slab is derived from the bulk cubic space group, *Fm*3*n*. The (1×1) geometries contain one water molecule per NaCl unit cell. The (2×1) and (4×2) structures required supercells containing two and 12 waters, respectively. The PHF method constructs crystalline orbitals from a linear combination of atomic orbitals. A mixed-split valence basis set, optimized for NaCl bulk,³² was used to describe the NaCl slab and was of the form 8-511G on sodium and 86-311G on chlorine. As in the earlier calculations on the water/MgO interface,^{23,24} the standard Pople 6-31d set³³ was used for water. The parameters controlling the tolerances used

in the evaluation of the infinite Coulomb and exchange series were 6, 6, 6, 14. These parameters have been shown to result in high numerical accuracy.^{27,31} Full analytic geometry optimizations are not possible using CRYSTAL; hence, single energy point calculations (along selected coordinates) were used to probe the potential energy surface in the vicinity of local minima. In most of the calculations the water–oxygen positions were held fixed in their empirically determined positions and the water–water orientations were varied along specific reaction coordinates.

The binding energies E_{bind} were computed with respect to an isolated gas-phase water molecule [$E_{\text{H}_2\text{O}(\text{g})}$] and a clean NaCl(001) surface, according to

$$E_{\text{bind}} = E_{(\text{water/NaCl})} - [E_{\text{H}_2\text{O}(\text{g})} + E_{\text{NaCl}}] \quad (1)$$

Comparisons of the formation energy of a periodic net of water molecules, in the absence of the surface, to the overall binding energy give insight into the relative contributions of water–water and water–surface interactions to the formation of the interface. The energetics of chemidissociation of water on flat NaCl(100) were determined from the difference in energy between the “fully hydroxylated” surface–hydroxyl group on every cation site and a hydrogen on every anion—and an isolated water molecule and the clean surface.^{23,24}

Calculations of the water dimer binding energy were used to estimate the accuracy of the PHF calculations. Using the basis set described above, the dimer binding energy at the Hartree–Fock level of theory was 5.0 kcal/mol. This value is in (fortuitously) good agreement with calculations done at higher levels of theory which report (D_e) binding energies of 4.65 to 5.05 kcal/mol.^{34–36} The empirical value is reported to be 5.4 ± 0.7 kcal/mol.^{37,38} Corrections to the binding energies due to basis set superposition errors (BSSE) are expected to be small at this level of theory. An estimate of the BSSE was made from calculations on the water dimer which showed that the BSSE contribution to the binding energy is 0.2 kcal/mol.

CRYSTAL uses an a posteriori density functional theory (DFT) method to estimate correlation energies from the fully converged PHF charge density. We report the PHF and PHF+correlation-corrected binding energies using three DFT functionals, Colle–Salvetti (CS)³⁰, Perdew^{39,40} (P86), and Perdew⁴¹ (P91). Similar calculations were performed on the water/MgO(001) interface.²³ Without more extensive and unambiguous empirical data it is not possible to assess the inherent accuracy of the correlation corrections to the PHF binding energies. However, the computed PHF and the PHF+correlation energetics have been shown to bracket a range of binding energies that are consistent with the empirical data in this study and in earlier work.²³

III. Results

A. (1×1) Monolayer. An example (1×1) monolayer structure is shown in Figure 1. The distance (*z*) between the water and the surface was optimized, fixing the water orientation and (*x,y*) position to be one of the several shown in Table 2, for several water/surface orientations. The monolayer structures contain one distinct water molecule for every surface NaCl unit. The binding energies and equilibrium distances for several orientations of the water with respect to the surface are shown in Table 2. In these configurations, either the water oxygens are located directly over a sodium site (Table 2a–c) or one or both hydrogens are directly over a chlorine site (parts d and e of Table 2, respectively). Of the structures shown in Table 2, the energetically favorable configuration occurs when the

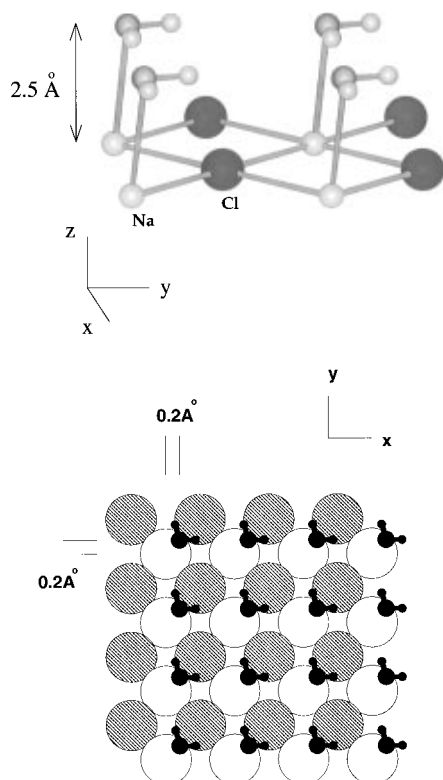


Figure 1. A (1×1) monolayer structure depicted in three-dimensional perspective (a, top), and in top view (b, bottom). The water dipole is parallel to the surface plane with the oxygen atom located above the sodium atom but shifted by 0.2 Å in both *x* and *y* coordinates. The separation between the surface plane and the oxygen atom center is 2.5 Å.

molecular dipole is aligned parallel to the surface plane, with the oxygens over the sodium sites (Table 2a). This geometry is very similar to the minimum energy configuration reported for water on MgO(001).²⁶ The computed binding energy in this configuration is 9.8 kcal/mol at the PHF level and 11.6–13.4 with correlation corrections. Much weaker binding occurs for geometries with the water in the vicinity of the chloride sites.

The relative contribution of “water–water” ($E_{\text{water–water}}$) vs “water–surface” ($E_{\text{water–surface}}$) interaction energies to the total binding energy (E_{bind}) (as computed by eq 1) for a given geometry can be estimated from the total binding energy (E_{bind}) and the interaction energy of the net of water molecules. The latter quantity is obtained from the total energy of a two-dimensional net of water molecules (E_{net}), arranged at a geometry corresponding to the monolayer spacing, without the surface present.

$$E_{\text{bind}} = E_{\text{water–surface}} + E_{\text{water–water}} \quad (2)$$

where

$$E_{\text{water–water}} = E_{\text{net}} - E_{\text{H}_2\text{O(g)}} \quad (3)$$

The water–water interaction energies and their corresponding monolayer geometries are shown in Table 2. These data indicate that the relative contributions to the binding energy are very dependent on the geometry. All of these structures, except that in part b, have an attractive water–water interaction. For the most stable geometry (Table 2a) the water–surface interaction is the dominant contribution to the binding energy (~70%).

The recent He scattering measurements of Bruch et al.¹⁰ are used to obtain a fitted isosteric heat of adsorption for the 2D

TABLE 2: The (1×1) Monolayer Geometries (PHF) and Calculated Adsorbate/Surface Binding Energies and Interaction Energies of the Water Nets without the Surface Present (PHF and with Correlation Corrections)^a

Geometry	Binding Energy (kcal/mol)	Water–Water Interaction Energy (kcal/mol)
a	$R_{\text{w-surf}} = 2.5 \text{ Å over Na}$	
	PHF = -9.8	PHF = -3.4
	PHF + CS = -13.4	PHF + CS = -3.6
	PHF + P86 = -12.3	PHF + P86 = -3.4
	PHF + P91 = -11.6	PHF + P91 = -3.4
b	$R_{\text{w-surf}} = 2.3 \text{ Å over Na}$	
	PHF = -3.4	PHF = +3.5
	PHF + CS = -7.5	PHF + CS = +3.5
	PHF + P86 = -6.2	PHF + P86 = +3.8
	PHF + P91 = -5.3	PHF + P91 = +3.7
c	$R_{\text{w-surf}} = 3.7 \text{ Å over Cl}$	
	PHF = -2.5	PHF = -0.6
	PHF + CS = -3.7	PHF + CS = -0.7
	PHF + P86 = -3.3	PHF + P86 = -0.6
	PHF + P91 = -3.2	PHF + P91 = -0.6
d	$R_{\text{w-surf}} = 3.4 \text{ Å (oxygen to surface plane)}$	
	PHF = -1.7	PHF = -0.6
	PHF + CS = -2.8	PHF + CS = -0.7
	PHF + P86 = -2.3	PHF + P86 = -0.6
	PHF + P91 = -2.1	PHF + P91 = -0.6
e	$R_{\text{w-surf}} = 3.5 \text{ Å (oxygen to surface plane)}$	
	PHF = -3.7	PHF = -1.8
	PHF + CS = -5.1	PHF + CS = -1.9
	PHF + P86 = -4.7	PHF + P86 = -1.8
	PHF + P91 = -4.5	PHF + P91 = -1.8

^a Negative binding energies denote attractive interactions, and positive numbers indicate repulsive interactions. The PHF equilibrium distances ($R_{\text{w-surf}}$) are defined between the oxygen and the plane of the surface. All of these calculations were run using a three-layer slab NaCl(100).

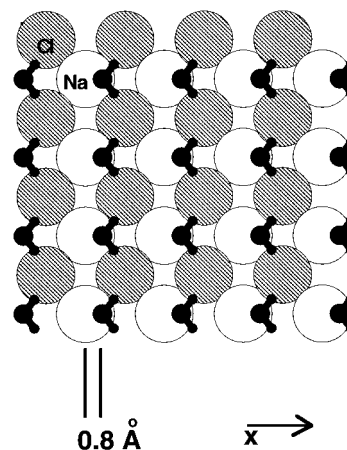


Figure 2. The (1×1) structure determined by Bruch et al.¹⁰ using helium scattering as a probe (top view). The water dipoles are aligned parallel to the *x* coordinate and nearly parallel to the NaCl(100) surface plane. The oxygen atoms are located above the sodium atom centers but shifted by 0.8 Å.

condensed phase of 14 ± 1 kcal/mol and a single-molecule heat of adsorption of 15 ± 1 kcal/mol. Our calculated binding energies are analogous to fitted isosteric heat of adsorption values because they include both water–water and water–surface contributions to the binding energy (see eq 1). Bruch et al.¹⁰ assign the 2D condensed phase to be a (1×1) structure with the water dipoles nearly parallel to the surface plane and the water oxygens moved off the sodium centers by 0.8 Å as shown in Figure 2. Our ab initio calculations confirm that displacing the water oxygen from the sodium centers lowers the energy. The computed minimum occurs when the waters

TABLE 3: Comparison of Monolayer Adsorbate/Surface Binding Energies and Interaction Energies of the Water Nets without the Surface Present for Three Coverages (100, 50, and 25%)^a

	percent water coverage	binding energy (kcal/mol)	water–water interaction energy (kcal/mol)
Optimized Planar Water over Sodium: Figure 1 Geometry			
(1×1)	100	PHF = −10.8	PHF = −3.4
		PHF + CS = −15.1	PHF + CS = −3.6
		PHF + P86 = −14.0	PHF + P86 = −3.4
(2×2)	50	PHF + P91 = −13.1	PHF + P91 = −3.4
		PHF = −8.3	PHF = −0.6
		PHF + CS = −12.4	PHF + CS = −0.7
(2×2)	25	PHF + P86 = −11.3	PHF + P86 = −0.7
		PHF + P91 = −10.4	PHF + P91 = −0.7
		PHF = −8.0	PHF = <−0.5
		PHF + CS = −12.1	PHF + CS = <−0.5
		PHF + P86 = −11.0	PHF + P86 = <−0.5
		PHF + P91 = −10.1	PHF + P91 = <−0.5
Planar Water over Sodium Bruch Geometry Displaced 0.6 Å			
(1×1)	100	PHF = −10.4	PHF = −1.5
		PHF + CS = −15.6	PHF + CS = −1.6
		PHF + P86 = −14.5	PHF + P86 = −1.4
(2×2)	50	PHF + P91 = −13.5	PHF + P91 = −1.5
		PHF = −10.0	PHF = −0.9
		PHF + CS = −15.0	PHF + CS = −0.8
(2×2)	25	PHF + P86 = −14.0	PHF + P86 = −0.8
		PHF + P91 = −12.9	PHF + P91 = −0.8
		PHF = −9.3	PHF = <−0.5
		PHF + CS = −12.1	PHF + CS = <−0.5
		PHF + P86 = −11.0	PHF + P86 = <−0.5
		PHF + P91 = −10.1	PHF + P91 = <−0.5
Water over Sodium: Table 2b Geometry			
(1×1)	100	PHF = −3.3	PHF = +3.5
		PHF + CS = −7.5	PHF + CS = +3.5
		PHF + P86 = −6.1	PHF + P86 = +3.8
(2×2) parallel	50	PHF + P91 = −5.3	PHF + P91 = +3.7
		PHF = −6.0	PHF = +1.7
		PHF + CS = −10.2	PHF + CS = +1.8
(2×2) hatch	50	PHF + P86 = −9.0	PHF + P86 = +1.8
		PHF + P91 = −8.0	PHF + P91 = +1.8
		PHF = −6.3	PHF = +1.4
(2×2)	25	PHF + CS = −10.5	PHF + CS = +1.5
		PHF + P86 = −9.3	PHF + P86 = +1.5
		PHF + P91 = −8.4	PHF + P91 = +1.5
		PHF = −7.7	PHF = +0.5
		PHF + CS = −12.0	PHF + CS = +0.6
		PHF + P86 = −10.7	PHF + P86 = +0.6
		PHF + P91 = −9.8	PHF + P91 = +0.6
Water over Chlorine: Table 2e Geometry			
(1×1)	100	PHF = −3.5	PHF = −1.8
		PHF + CS = −4.7	PHF + CS = −1.9
		PHF + P86 = −4.4	PHF + P86 = −1.8
(2×2)	50	PHF + P91 = −4.2	PHF + P91 = −1.8
		PHF = −2.4	PHF = −0.7
		PHF + CS = −3.5	PHF + CS = −0.7
(2×2)	25	PHF + P86 = −3.2	PHF + P86 = −0.7
		PHF + P91 = −3.0	PHF + P91 = −0.7
		PHF = −2.0	PHF = <−0.5
		PHF + CS = −3.0	PHF + CS = <−0.5
		PHF + P86 = −2.8	PHF + P86 = <−0.5
		PHF + P91 = −2.6	PHF + P91 = <−0.5

^a Negative binding energies denote attractive interactions, and positive numbers indicate repulsive interactions. All of these calculations were run using a one-layer slab NaCl(100).

are displaced by 0.6 Å, corresponding to a binding energy of 10.4 kcal/mol at the PHF level and 13.5–15.6 kcal/mol with correlation (see Table 3). Similar behavior is found when the waters are displaced from the sodium centers in the orientation shown in Figure 1. In this case the minimum energy occurs with displacements of 0.2 Å in both *x* and *y* (in-plane coordinates), with a corresponding binding energy of 10.8 kcal/mol at PHF and 13.1–15.1 kcal/mol with correlation. The computed energies and geometries are in good agreement with the experimental values.

The propensity of the NaCl(100) surface to dissociate water was also investigated. Our calculations indicate that the formation of a “fully hydroxylated” surface (corresponding to a hydroxyl group on each sodium and a hydrogen on each chloride) is endothermic. This is consistent with the Bruch et al. (ref 10) study which reports “no apparent effect of hydrolysis on the coherence length of the surface.” Earlier studies on the water/MgO(100) interface also showed that water dissociation was endothermic on flat terrace sites²³ but was energetically possible on low-coordinated defect sites (step edges and corners).²⁴

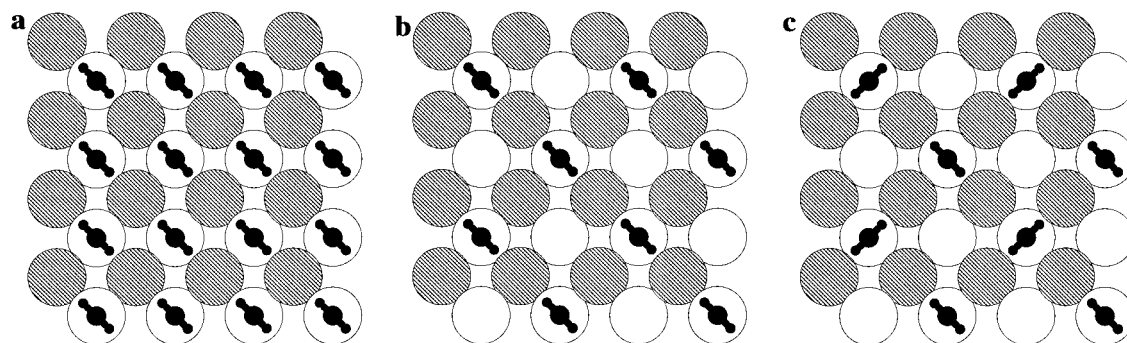


Figure 3. Trial structures with water dipoles oriented perpendicular to the NaCl(100) surface plane in top view. The oxygen atom centers are located directly above the sodium atom centers at a separation of 2.3 Å. A side view of this trial structure is presented in Table 2b. Part a represents a (1×1) structure at 100% coverage; hydrogen atoms are aligned along the *x* coordinate. Part b represents a (1×1) structure at 50% coverage; hydrogen atoms are aligned as in part a but the binding energy is decreased at the lower coverage due to a reduction of the water–water repulsion. Part c represents a (1×1) structure at 50% coverage; hydrogen atoms are aligned in a hatched configuration to optimize water–water interactions.

We probed the energetics as a function of coverage for 50% and 25% of a monolayer by creating supercells with one water for every two or four NaCl units, respectively. In these calculations the molecule–surface orientations were fixed at their high-coverage minimum positions. Table 3 shows the results of changes in coverage for four molecule/surface geometries. In the two configurations described above—the optimized geometry corresponding to the orientation shown in Figure 1 and the optimized “Bruch” geometry—and in the “chloride-site” geometry shown in Table 2e, the binding energies decrease with decreasing coverage. This is due to a reduction in the attractive water–water (dipole–dipole) interactions as the coverage is reduced. The water net interaction energies at 25% monolayer coverage are ~ 0.5 kcal/mol; therefore, the reported binding energies at low coverage are almost entirely due to water–surface interactions and, hence, are representative of the isolated molecule limit.

In contrast, when the molecular dipole is aligned perpendicular to the surface plane as shown in Figure 3 (corresponding to Table 2b), the binding energy increases with decreasing coverage. This effect was also observed in the molecular dynamics simulations of Wasserman et al.⁶ The perpendicular configurations are unfavorable at high coverages because of the strong water–water (dipole–dipole) repulsive interactions; these are reduced as the molecules are separated at the lower coverages. The energetics of two water arrangements at the 50% monolayer coverage (shown in Figure 3b,c) were computed. The slight decrease in the binding energy occurs in the hatched configuration (Figure 3c) due to the more favorable water–water interactions. A similar effect was also observed in calculations of water on MgO(100).²³

B. (2×1) Monolayer. Figure 4 shows the geometry of a proposed (2×1) monolayer geometry. Two waters are present for every two NaCl units. The orientations of the waters with respect to the surface were set to correspond to the equilibrium monolayer (1×1) geometries for waters bound over the sodium and chloride sites. The oxygen–oxygen distance in this geometry is 3.65 Å. This geometry was investigated because it relates the (1×1) monolayer geometries with the (4×2) bilayer geometries described below. However, the formation energy of this structure was found to be endothermic.

C. (4×2) Bilayers. The adsorption of water on thin films of NaCl(100), grown on Ge(100) substrates, was probed with UPS, XPS, and LEED.^{4,5} These experiments indicate a c(4×2) bilayer structure, with the water oxygens arranged in a hexagonal net on the surface with six symmetry distinct waters per NaCl supercell (consisting of four NaCl units). The water density in the bilayer is 150% that of the (1×1) monolayer. The bilayer

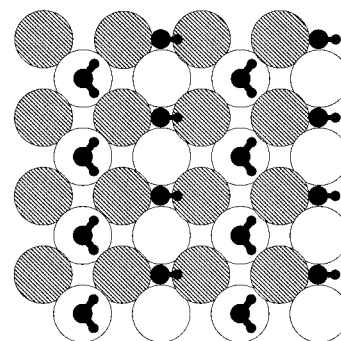


Figure 4. Trial structure of a (2×1) monolayer geometry designed as a possible “transition state” between (1×1) and (4×2) structures. This structure was found to be unbound (endothermic) and is therefore not a possible transition state.

consists of a tightly packed net with the waters arranged in two “layers” with different oxygen–surface distances. The oxygen positions relative to the underlying NaCl lattice are shown in Figure 5, with the “upper” and “lower” oxygens shaded in black and gray, respectively (Figure 5b). The positions of the hydrogens have not been determined from experiment, however, the orientations of the waters has been modeled using classical simulations.^{6,11}

We constructed several (4×2) geometries based on the proposed models and computed the *ab initio* energetics. Initially, we fixed the upper and lower oxygen–surface distances at 3.5 and 2.5 Å, respectively, as shown in Figure 5b. These values were determined independently from the equilibrium positions computed for the corresponding monolayer structures. The geometries and energetics for 10 bound configurations are shown in Table 4. These geometries are based on one of the three in-plane structures shown in Figures 6–8. The supercell containing 12 waters and eight NaCl units is outlined in Figure 6. The structure in Table 4a corresponds to Figure 6 and results from combining the minimized monolayer geometries for water bound over the sodium and chloride sites. Figure 7 results when the planar water molecules (over the sodium sites) are allowed to tilt up, thus permitting the formation of a water–water hydrogen-bonded network. The structures in parts b and c of Table 4 correspond to Figure 7 with tilt angles of 14 and 20°, respectively. A tilt angle of 14° allows the surface–oxygen hydrogen bond to have a tetrahedral-like structure. The more energetically favorable geometry has a 20° tilt which allows the lower water O–H bonds to point directly at the neighboring oxygen atoms in the upper waters of the bilayer.

It is possible to construct more extensive hydrogen-bonded networks of waters on this surface. One way to do this within

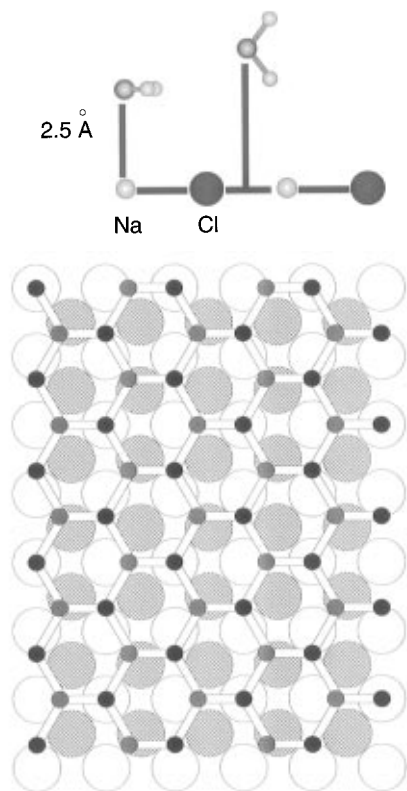


Figure 5. Proposed hexagonal bilayer structure for water on NaCl surface: (a, top) side view showing the location and orientation of distinct water molecules and the NaCl surface to oxygen atom center separations of 2.5 and 3.5 Å, (b, bottom) top view of the hexagonal (4×2) structure showing the “upper” and “lower” oxygen layers in black and gray shading, respectively.

the (4×2) bilayer geometry is to fix one of the upper water O—H bonds to be aligned along the surface normal, perpendicular to the surface. The remaining water O—H points toward a neighboring oxygen atom in the lower layer of waters of the bilayer. Hexagons of waters with alternating counterclockwise—clockwise hydrogen bonding can be assembled into a larger hexagon as shown in Figure 8 and Table 4d–g. The structure in Table 4d has the lower waters in the bilayer fixed in a planar geometry, with the upper waters having one OH bond pointed toward the surface. The configuration in Table 4e is similar to Table 4d, with the planar waters allowed to tilt up by 14° . In Table 4f,g the upper waters have one OH bond pointing away from the NaCl surface with the lower waters either tilted up by 14° (Table 4f) or planar (Table 4g). The most energetically favorable structure of this type is shown in Table 4g.

All of the geometries described up to this point fixed the oxygen—surface distances of the upper and lower waters in the bilayer and varied only the hydrogen positions (molecular orientations). The final set of geometries (Table 4h–j) are based on the structure shown in Figure 6, but the heights of the oxygen atoms were allowed to vary according to a scheme derived from the three-parameter pucker model for cyclohexane given by Cremer and Pople.⁴² They define three pucker parameters, an amplitude and two angles. Taken together these three parameters provide a simple way to describe the location of atoms in a six-membered ring. In our calculations the “pucker amplitude” was fixed and the angles were varied. Changes in the pucker angles caused variations in the oxygen—surface heights. These changes result in distortions away from a true bilayer geometry. These geometries are all lower in energy than the bilayer geometries described above. The lowest energy configuration with a binding energy of 9.6 kcal/mol is shown in Table 4k. In this geometry both pucker angles are set to about 45° .

IV. Discussion and Conclusions

These calculations indicate several energetically favorable arrangements for water on NaCl(100). The most stable monolayer geometry occurs with the molecular dipole aligned nearly parallel to the surface plane and the water bound in the vicinity of the sodium site with binding energies of 10–11 kcal/mol at the PHF level and 12–16 kcal/mol with correlation corrections. These values are in good agreement with the experimental values.¹⁰ Much weaker interactions occur in monolayer structures with the waters “hydrogen bonded” to the chloride sites. Small changes in the binding energy were observed when the in-plane angular orientation of the water was changed. This implies that there may be multiple local minima on the water—NaCl potential energy surface corresponding to similar (1×1) monolayer geometries. These structures could exist as separate domains on the surface. In the most stable structure, the dominant contribution (around 70%) to the binding energy comes from the water—surface interactions and the remaining 30% results from the water—water (dipole—dipole) interactions. However, the relative contributions of water—water and water—surface interactions to the overall binding energy is very dependent on the orientations of the waters. Much weaker interactions occur in monolayer structures with the waters “hydrogen bonded” to the chloride sites.

The overall binding energy in the parallel geometries is reduced as the coverage is decreased (to 50% or 25% of a monolayer) due to the decrease in water—water attraction at large separations. In contrast, the binding energy of the adsorbate—surface structure with the water dipole aligned perpendicular to the surface over a sodium site increases with decreasing surface coverage. This is because the water dipoles have a repulsive interaction in this configuration. At 25% of a monolayer the intermolecular separations are sufficient to reduce the water—water repulsion to <0.5 kcal/mol, thus increasing the overall PHF binding energy to around 8 kcal/mol. This value is close to the low-coverage parallel configuration PHF binding energies (8–9 kcal/mol), indicating that the isolated or low-coverage adsorbate—surface structures may be different from the full monolayer geometries. A similar result was observed in molecular dynamics simulations reported by Wasserman, et al.⁶

The (4×2) bilayers can be viewed (approximately) as a combination of two monolayer geometries; water parallel to the surface over sodium sites and water “hydrogen bonded” to chloride sites. The calculated binding energies for several proposed (4×2) bilayer geometries ranged from 5.6–9.6 kcal/mol at the PHF level to 8.0–14.5 kcal/mol with correlation corrections. These are similar to the experimental values reported by Folsh⁵ and to the computed (1×1) monolayer geometries. However, the (4×2) structures have 150% higher packing density, and hence, the formation energy per unit area is greater for the (4×2) structures. The increase in the water—water attraction energy at the higher (4×2) packing density (relative to the monolayer) stabilizes these structures. On the basis of the computed energetics, it is reasonable to expect that domains of (1×1) and (4×2) structures could coexist on NaCl(100), with their relative concentrations being dependent on sample conditions such as surface preparation technique, coverage, and temperature. The (4×2) geometries may become more stable as the coverage is increased, but the mechanism (reaction path) for converting between (1×1) and (4×2) geometries is as yet undetermined.

Our calculations also indicate that the most energetically favorable of the (4×2) structures occurs when the “bilayer” model is relaxed (e.g. in structures with more than two oxygen—

TABLE 4: Calculated Water Binding Energies for Periodic Hartree–Fock and Correlation-Corrected PHF Calculations for the 4×2 Water Bilayer Structures^a

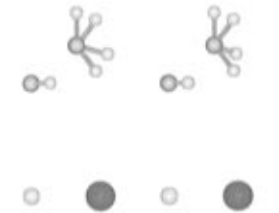
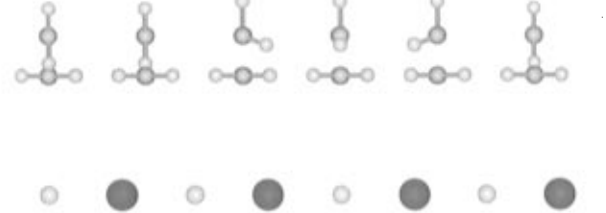
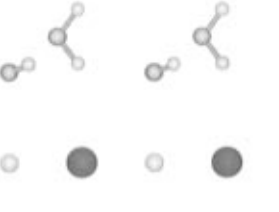
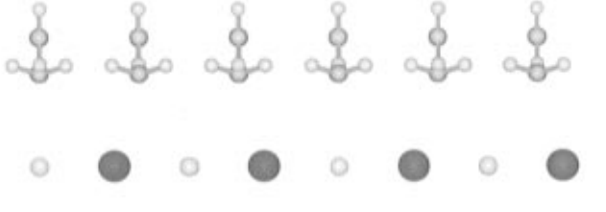
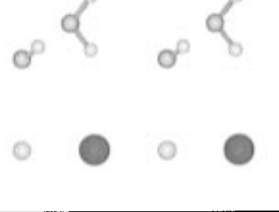
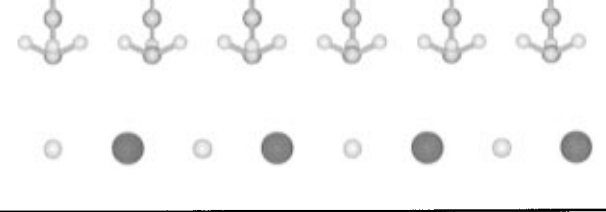
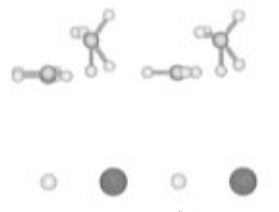
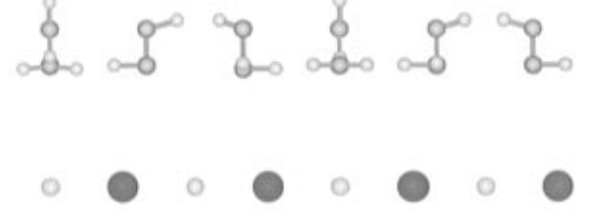

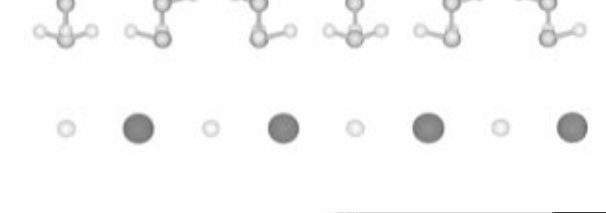
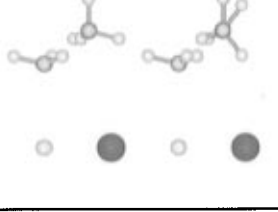
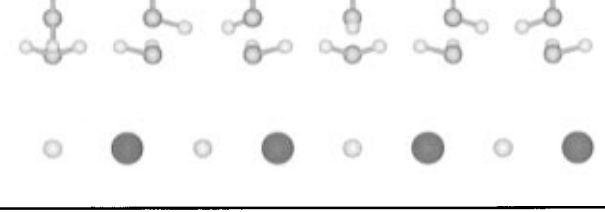
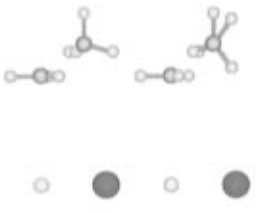

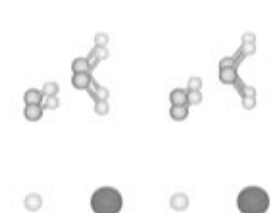
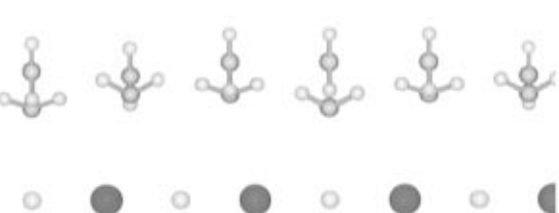

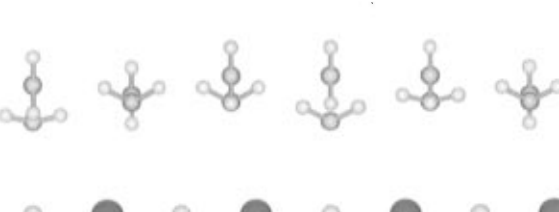

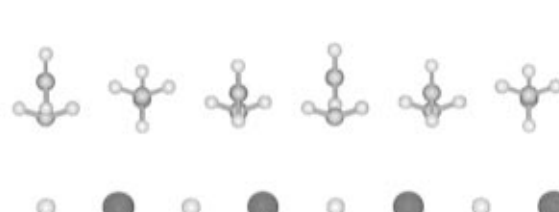
(case) Energy kcal/mol		
(a) pHF = -6.63 pHF+CS = -11.00 pHF+P86 = -11.64 pHF+P91 = -10.69 Refer Figure 6 no "tilt"		
(b) pHF = -8.75 pHF+CS = -13.23 pHF+P86 = -12.14 pHF+P91 = -11.18 Refer Figure 7 14 degree "tilt"		
(c) pHF = -9.05 pHF+CS = -13.52 pHF+P86 = -12.41 pHF+P91 = -11.45 Refer Figure 7 20 degree "tilt"		
(d) pHF = -5.59 pHF+CS = -10.13 pHF+P86 = -9.01 pHF+P91 = -8.01 Refer Figure 8		
(e) pHF = -7.70 pHF+CS = -12.31 pHF+P86 = -11.21 pHF+P91 = -10.23 Refer Figure 8 14 degree "tilt"		
(f) pHF = -8.08 pHF+CS = -12.54 pHF+P86 = -11.44 pHF+P91 = -11.49 Refer Figure 8 14 degree "tilt"		

TABLE 4 (Continued)

(g) $\text{pHF} = -8.28$ $\text{pHF} + \text{CS} = -12.73$ $\text{pHF} + \text{P86} = -11.64$ $\text{pHF} + \text{P91} = -10.69$ Refer Figure 8		
(h) $\text{pHF} = -9.27$ $\text{pHF} + \text{CS} = -13.41$ $\text{pHF} + \text{P86} = -12.30$ $\text{pHF} + \text{P91} = -11.43$		
(i) $\text{pHF} = -9.33$ $\text{pHF} + \text{CS} = -13.55$ $\text{pHF} + \text{P86} = -12.45$ $\text{pHF} + \text{P91} = -11.56$		
(j) $\text{pHF} = -9.58$ $\text{pHF} + \text{CS} = -14.51$ $\text{pHF} + \text{P86} = -13.47$ $\text{pHF} + \text{P91} = -12.45$		

^a Two side views (in the xz and yz planes, respectively) of the 4×2 water bilayer structure are presented for each structure. Negative binding energies denote attractive interactions, and positive numbers indicate repulsive interactions. The "tilt" angle refers to the water located over the sodium site.

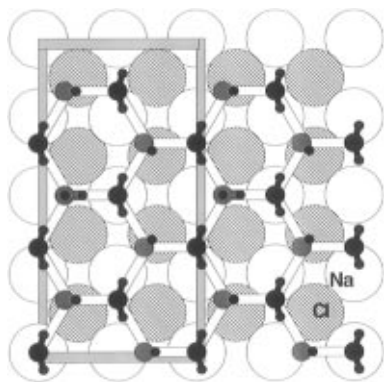


Figure 6. The (4×2) supercell containing 12 waters and eight NaCl units is outlined by the gray rectangle. The structure is a combination of the minimized geometries of water positioned over sodium and chloride sites and corresponds to the structure presented in Table 4a.

surface distances). These structures still have the oxygens in a (4×2) lattice relative to the NaCl surface, but they are no longer "bilayers", since they have a range of oxygen-surface distances. This "disordering" of the oxygen-surface positions and the

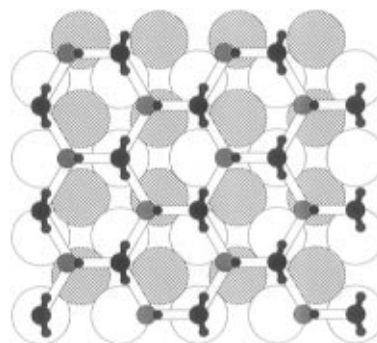


Figure 7. A (4×2) structure containing 12 waters and eight NaCl units. The structure is similar to Figure 6 except the water molecules are allowed to tilt off parallel from the NaCl plane to form a water-water hydrogen-bonded network. The corresponding structures, tilted by angles of 14 and 20°, are presented in parts b and c of Table 4, respectively.

possibility of forming of domains of different (4×2) or (1×1) structures on the surface may be responsible for the diffuseness observed in the LEED data.^{4,5}

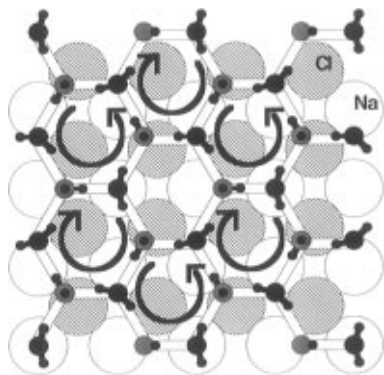


Figure 8. A larger hexagonal structure is constructed of smaller water "hexagons". The smaller hexagons contain water structures of alternating counterclockwise–clockwise hydrogen bonding. The corresponding structures are presented in Table 4d–g.

Acknowledgment. We gratefully acknowledge helpful discussions and consultations with Drs. Stephen Joyce, Scott Smith, Michael Stirniman, Gregory Schenter of PNNL, and Prof. George Ewing (Department of Chemistry, Indiana University). Pacific Northwest National Laboratory is a multiprogram laboratory operated for the U.S. Department of Energy (USDOE) by Battelle Memorial Institute under Contract No. DE-AC06-76RLO 1830. The authors were supported by the Division of Chemical Sciences of the Office of Basic Energy Sciences, USDOE, and D.P.T. was supported by the Northwestern College and University Association for Science (Washington State University) under Grant No. DE-FG06-89ER-75522 with the USDOE. We would like to thank the Scientific Computing Staff, Office of Energy Research, USDOE, for a grant of computing time at the National Energy Research Scientific Computing Center.

References and Notes

- Thiel, P.; Madey, T. E. *Surf. Sci. Rep.* **1987**, 7, 211.
- Ewing, G. E. *Acc. Chem. Res.* **1992**, 25, 292.
- Barracough, P. B.; Hall, P. G. *Surf. Sci.* **1974**, 46, 393.
- Folsch, S.; Henzler, M. *Surf. Sci.* **1991**, 247, 269.
- Folsch, S.; Stock, A.; Henzler, M. *Surf. Sci.* **1992**, 264, 65.
- Wassermann, B.; Mirbt, S.; Reif, J.; Zink, J. C.; Matthias, E. *J. Chem. Phys.* **1993**, 98, 10049.
- Dai, D. J.; Peters, S. J.; Ewing, G. E. *J. Phys. Chem.* **1995**, 99, 10299.
- Ichikawa, K.; Yamada, M. *J. Phys.: Condens. Matter.* **1996**, 8, 4889.
- Stefanovich, E. V.; Truong, T. N. *Chem. Phys. Lett.*, submitted.
- Bruch, L. W.; Glebov, A.; Toennies, J. P.; Weiss, H. J. *Chem. Phys.* **1995**, 103, 5109.
- Picaud, S.; Girardet, C. *Chem. Phys. Lett.* **1993**, 209, 340.
- Laux, J. M.; Hemminger, J. C.; Finlayson-Pitts, B. J. *Geophys. Res. Lett.* **1994**, 21, 1623.
- Keene, W. C.; *et al.* *Global Biogeochem. Cycles* **1990**, 4, 407.
- Finlayson-Pitts, B. J. *Res. Chem. Int.* **1993**, 19, 235.
- Finlayson-Pitts, B. J.; Exell, M. J.; Pitts, J. N. *Nature* **1989**, 337, 241.
- Henrich, V. E.; Cox, P. A. *The Surface Science of Metal Oxides*; Cambridge University Press: New York, 1994.
- Goodman, D. W. Personal communication on work in progress, 1996.
- Rowland, B.; Kadagather, N. S.; Devlin, J. P.; Buch, V.; Feldman, T.; Wojcik, M. J. *J. Chem. Phys.* **1995**, 102, 8328.
- Hermansson, K.; Soeren, K.; Lindgren, J. *J. Chem. Phys.* **1991**, 95, 7486.
- Ojamae, L.; Hermansson, K. *J. Phys. Chem.* **1994**, 98, 4271.
- Wojcik, M. J.; Buch, V.; Devlin, J. P. *J. Chem. Phys.* **1993**, 99, 2332.
- Ewing, G. In *Adsorption on Ordered Surfaces of Ionic Solids and Thin Films*; Umbach, E., Freund, H.-J., Eds.; 57 Springer-Verlag: Berlin, 1993.
- Scaemhorn, C. A.; Hess, A. C.; McCarthy, M. I. *J. Chem. Phys.* **1993**, 99, 2786.
- Scaemhorn, C. A.; Harrison, N. M.; McCarthy, M. I. *J. Chem. Phys.* **1994**, 101, 1547.
- Chacon-Taylor, M. R.; McCarthy, M. I. *J. Phys. Chem.* **1996**, 100, 7610.
- McCarthy, M. I.; Schenter, G. K.; Scaemhorn, C. A.; Nicholas, J. B. *J. Phys. Chem.* **1996**, 100, 16989.
- Pisani, C.; Dovesi, R.; Roetti, C. *Hartree–Fock Ab Initio Treatment of Crystalline Systems*; Springer-Verlag: New York, 1988.
- Causa, M.; Dovesi, R.; Pisani, C.; Colle, R.; Fortunelli, A. *Phys. Rev. B* **1987**, 36, 891.
- Causa, M.; Colle, R.; Fortunelli, A.; Dovesi, R.; Pisani, C. *Phys. Scr.* **1988**, 38, 194.
- Colle, R.; Salvetti, D. *Theor. Chim. Acta* **1975**, 37, 329.
- Dovesi, R.; Saunders, V. R.; Roetti, C. *CRYSTAL92 Users Manual*; Universita di Torino and SERC Daresbury Laboratory: Torino, Italy, and Daresbury, U.K., 1992.
- Apra, E.; Causa, M.; Prencipe, M.; Dovesi, R.; Saunders, V. R. *J. Phys.: Condens. Matter.* **1993**, 5, 2969.
- Hehre, W. J.; Radom, L.; Schleyer, P. v. R.; Pople, J. A. *Ab Initio Orbital Theory*; John Wiley and Sons: New York, 1986.
- Mas, E. M.; Szalewicz, K. *J. Chem. Phys.* **1996**, 104, 7606.
- Feyereisen, M. W.; Feller, D. F.; Dixon, D. A. *J. Phys. Chem.* **1996**, 100, 2993.
- Xantheas, S. S.; Dunning, T. H., Jr. *J. Chem. Phys.* **1993**, 99, 8774.
- Curtiss, L. A.; Frurip, D. J.; Blander, M. J. *Chem. Phys.* **1979**, 71, 2703.
- Reimers, J.; Watts, R.; Klein, M. *Chem. Phys.* **1982**, 64, 95.
- Perdew, J. P. *Phys. Rev. B* **1986**, 34, 7406.
- Perdew, J. P. *Phys. Rev. B* **1986**, 33, 8822.
- Perdew, J. P. *Unified Theory of Exchange and Correlation Beyond the Local Density Approximation*; Nova Science: New York, 1991.
- Cremer, D.; Pople, J. A. *J. Am. Chem. Soc.* **1975**, 97, 1354.